Open Access

OBM Transplantation

LIDSEN Publishing Inc.

Original Research

The P2X7 Receptor Antagonist AZ10606120 Does Not Alter Graft-Versus-Host Disease Development and Increases Serum Human Interferon-γ in a Humanized Mouse Model

Nicholas J. Geraghty [1, 2], Amal Elhage [1, 2], Peter Cuthbertson [1, 2], Debbie Watson [1, 2], Ronald Sluyter [1, 2, *]

1. Illawarra Health and Medical Research Institute, Wollongong, NSW, 2522, Australia; E-Mails: geraghty@uow.edu.au; ae880@uowmail.edu.au; cpeter@uow.edu.au; dwatson@uow.edu.au; rsluyter@uow.edu.au
2. Molecular Horizons and School of Chemistry and Molecular Bioscience, University of Wollongong, Wollongong, NSW, 2522, Australia

* **Correspondence:** Ronald Sluyter; E-Mail: rsluyter@uow.edu.au

Academic Editor: Martin Guimond

Special Issue: Allogeneic Stem Cell Transplantation

OBM Transplantation
2022, volume 6, issue 3
doi:10.21926/obm.transplant.2203166

Received: June 06, 2022
Accepted: August 31, 2022
Published: September 06, 2022

Abstract

Allogeneic hematopoietic stem cell transplantation is a curative therapy for hematological malignancies, but its efficacy is limited by graft-versus-host disease (GVHD). This life-threatening disorder develops when donor (graft) immune cells cause inflammatory damage to recipient (host) tissues. The immune cell receptor channel P2X7 and its ligand adenosine 5'-triphosphate (ATP) have been implicated in GVHD pathogenesis. Therefore, this signaling axis represents a potential therapeutic target. This study aimed to investigate if the specific P2X7 antagonist AZ10606120 (AZ10) could prevent GVHD development in a preclinical, humanized mouse model, in which NOD.Cg-*Prkdc*^{scid} *Il2rg*^{tm1Wjl}/SzJ (NSG) mice are injected with human peripheral blood mononuclear cells (hPBMCs). Flow cytometric measurements of ATP-induced cation dye uptake revealed that AZ10 blocked P2X7 activity in human RPMI 8226 multiple myeloma cells (IC_{50} of 1 ± 1 nM) and murine RAW 264.7 macrophages (IC_{50} of 3 ± 1

nM), as well as primary donor $CD4^+$ and $CD8^+$ T cells. However, AZ10 (2 mg/kg), injected intraperitonealy (i.p.) daily for the first 10 days post-hPBMC injection, did not reduce clinical or histological GVHD development in mice. AZ10 did not impact engraftment of human leukocytes, predominantly $CD4^+$ and $CD8^+$ T cells. However, AZ10 increased serum human interferon gamma (hIFN-γ) concentrations, with $CD8^+$ T cells being the main hIFN-γ producing T cell subset. In conclusion, this study suggests a role for P2X7 activation in impairing hIFN-γ production during GVHD pathogenesis, with the use of P2X7 blockade as a therapeutic strategy warranting further investigation.

Keywords
Graft-versus-host disease; xenogeneic graft-versus-host disease; P2X7 receptor; purinergic receptor; P2X7 antagonist; cytokine; humanized mice

1. Introduction

Allogeneic hematopoietic stem cell transplantation (allo-HSCT) is a curative therapy for hematopoietic malignancies. Allo-HSCT aims to eradicate malignant cells and to reconstitute the immune system of the recipient to prevent disease relapse [1]. However, a common complication of allo-HSCT is graft-versus-host disease (GVHD), which occurs in 30-50% of recipients. GVHD arises when donor (graft) T cells mount an inflammatory immune response against the recipient (host), damaging target tissues including the liver, skin, and gastrointestinal (GI) tract [2]. Despite advances in the understanding of GVHD pathogenesis there is no effective treatment [3], highlighting the need for new therapies.

The P2X7 receptor is an extracellular adenosine 5'-triphosphate (ATP)-gated receptor channel present on the cell surface of immune cells including antigen presenting cells (APCs) and T cells [4], cell types central in the development of GVHD [5]. To date various studies have established a role for the ATP-P2X7 signaling axis in the development of GVHD [6]. Intraperitoneal (i.p.) injections of the ATP-degrading enzyme, apyrase, revealed a role for extracellular ATP in the development of GVHD in an allogeneic mouse model of GVHD [7]. Moreover, the injection of the non-selective P2X7 antagonist pyridoxalphosphate-6-azophenyl-2',4'-disulfonic acid (PPADS) or the more selective P2X7 antagonist KN-62 (both i.p. daily, days 0-10) in two different allogeneic mouse models revealed a role for P2X7 activation in this process [7]. In this same study, the use of *P2rx7* deficient bone marrow chimeras indicated a role for P2X7 on host but not donor APCs in GVHD development [7]. More recently, use of the selective P2X7 antagonist A-438079 (daily, days 0-10 i.p.), confirmed a role for P2X7 activation in the development of GVHD in an allogeneic mouse model [8].

To extend the above findings from allogeneic mouse models of GVHD to humans, our group has been investigating the ATP-P2X7 signaling axis in a humanized mouse model of GVHD [9]. In this model, NOD.Cg-*Prkdc*^{scid} *Il2rg*^{tm1Wjl}/SzJ (NSG) mice are injected with human peripheral blood mononuclear cells (hPBMCs) and develop lethal GVHD from 4 weeks [10]. Injection of the non-selective P2X7 antagonist Brilliant Blue G (BBG) in this model (i.p. daily, days 0-10) reduced clinical GVHD development and histological liver GVHD, which corresponded with a decrease in serum human interferon (hIFN)-γ [11]. While the earlier study revealed that BBG injected i.p. every second

day (days 0, 2, 4, 6 and 8) reduced liver GVHD and serum hIFN-γ but not clinical GVHD in this model [10]. Moreover, i.p. injection of αβ-methylene ATP, which inhibits CD39/CD73, theoretically leading to increased extracellular ATP concentrations [12], worsened GVHD in humanized NSG mice [13]. Collectively, these studies support a role for the ATP-P2X7 signaling axis in GVHD development in humanized mice. However, the use of BBG, which is a non-selective P2X7 antagonist [14], in these studies remained a limitation. Thus, use of a selective P2X7 antagonist is required to confirm a role for P2X7 in the development of GVHD in this model.

AZ10606120 (AZ10) is a selective antagonist of P2X7 [15, 16], capable of binding to the allosteric binding pocket of this receptor [17] to which several other non-competitive P2X7 antagonists can also bind [18-20]. AZ10 can impair endogenous and recombinant P2X7 with a half-maximal inhibitory concentration (IC_{50}) of ~10 nM [17, 21]. Notably, i.p. injection of this compound (2 mg/kg) for four consecutive days attentuated endotoxin-induced depression in mice [22], while i.p. injection of AZ10 (5 mg/kg) every second day for 20 days reduced pancreatic tumor growth in mice [23]. Therefore, the current study investigated whether AZ10 could reduce GVHD progression in a humansed mouse model of GVHD. Contrary to our hypothesis, AZ10 (2 mg/kg i.p. daily, days 0-10) did not reduce GVHD and unexpectedly increased serum hIFN-γ in this humanized mouse model.

2. Materials and Methods

2.1 Cells

Human RPMI 8226 multiple myeloma and murine RAW 264.7 macrophage cell lines were obtained and cultured as described [24], using RPMI 1640 medium (Thermo Fisher Scientific, Waltham, USA) containing 2 mM L-glutamine (Thermo Fisher Scientific) and 10% fetal calf serum (FCS) (Bovogen Biologics, Keilor East, Australia). Cell lines were checked for *Mycoplasma spp.* infections using a MycoAlert™ Mycoplasma detection kit (Lonza; Basel, Switzerland) as per the manufacturer's instructions and were routinely negative for *Mycoplasma spp.* hPBMCs were isolated by density centrifugation using Ficoll-Paque PLUS (GE Healthcare, Uppsala, Sweden) as described [10] and resuspended in Dulbecco's phosphate-buffered saline (PBS) (Thermo Fisher Scientific).

2.2 Ethics Statement

Experiments involving human blood and mice were approved by the Human Research Ethics Committee (Protocol HE12/290, approved 1 November 2012) and the Animal Ethics Committee (Protocol AE12/16, approved 25 October 2012) (University of Wollongong, Wollongong, Australia), respectively. Human blood and mice were used according to *The National Statement on Ethical Conduct in Human Research* and *The Australian Code for the Care and Use of Animals for Scientific Purposes* (National Health and Medical Research Council, Canberra, Australia), respectively.

2.3 ATP-induced YO-PRO-1^{2+} Uptake Assay

P2X7 activity was quantified by measuring ATP-induced YO-PRO-1^{2+} uptake as described [25]. Briefly, cells, washed and resuspended in NaCl medium (145 mM NaCl, 5 mM KCl, 5 mM glucose and 10 mM HEPES, pH 7.4), were incubated in the absence or presence of AZ10 (Tocris Biosciences, Bristol, UK) as indicated for 15 min at 37°C, and then incubated with 1 μM YO-PRO-1 iodide

(Molecular Probes, Eugene, USA) in the absence or presence of 100 µM ATP (Sigma-Aldrich, St Louis, USA) for 10 min. Incubations were stopped by addition of ice-cold NaCl medium containing 20 mM $MgCl_2$ ($MgCl_2$ medium) and centrifugation (300 × g for 3 min), and washed once in NaCl medium. Cells were incubated with fluorochrome-conjugated monoclonal antibodies (mAbs) (Table 1) as indicated for 15 min and washed once with NaCl medium. Data for RPMI 8226 and RAW 264.7 cells was collected using a BD Biosciences (La Jolla, USA) LSRII flow cytometer (band-pass filters: 515/20 for YO-PRO-1^{2+}, 586/15 for PE, 780/60 for PE-Cy7, 695/40 for PerCP-Cy5.5 and 670/30 for APC). Data for hPBMCs was collected using a BD Biosciences Fortessa X-20 flow cytometer (band-pass filters: 525/50 for YO-PRO-1^{2+}, 710/50 for BV711, 675/40 for PerCP-Cy5.5 and 780/60 for PE-Cy7). Fluorescence intensity of YO-PRO-1^{2+} uptake was analyzed using FlowJo software v8.7.1 (BD Biosciences).

Table 1 Monoclonal antibodies (BD Biosciences) used for flow cytometry.

Target	Host	Target	Fluorochrome	Clone
CD3	Mouse	Human	BV711 or PE	UCHT1
CD3	Mouse	Human	PerCP-Cy5.5	SK7
CD4	Mouse	Human	FITC	L200
CD4	Mouse	Human	PerCP-Cy5.5	SK3
CD45	Mouse	Human	FITC	HI30
CD45	Rat	Mouse	PerCP-Cy5.5	30-F11
CD56	Mouse	Human	APC	B159
CD8	Mouse	Human	PE or PE-Cy7	RPA-T8
IFN-γ	Mouse	Human	FITC	B27

Abbreviations: APC, allophycocyanin; BV, brilliant violet; CD, cluster of differentiation; Cy, cyanin; FITC, fluorescein isothiocyanate; IFN, interferon; PE, phycoerythrin: PerCP, peridinin chlorophyll protein

2.4 Humanized Mouse Model of Graft-versus-host Disease (GVHD)

A humanized mouse model of GVHD was used as described [26]. Briefly, female NSG mice aged 6-8 weeks (Australian BioResources, Moss Vale, Australia) were injected i.p. with 10 × 10^6 hPBMCs, isolated as above, in PBS on day 0. NSG mice were subsequently injected i.p. daily (days 0 to day 10) with PBS (saline) or AZ10 in PBS (2 mg/kg). At 3 weeks post-hPBMC injection, mice were checked for engraftment by immunophenotyping of tail vein blood. Mice were monitored for weight loss, survival, and clinical signs of GVHD using an established scoring system, giving a total clinical score out of 10 [10]. Mice were euthanized at humane endpoint (clinical score of ≥8 or a weight loss of ≥10%) or at the experimental endpoint (10 weeks post-hPBMC injection), according to the approved animal ethics protocol.

2.5 Immunophenotyping by Flow Cytometry

Tail vein blood (week 3) and spleen cells (endpoint) were obtained from mice and lysed with ammonium chloride potassium lysis buffer (150 mM NH_4Cl, 1 mM $KHCO_3$ and 0.1 mM Na_2CO_3) and

immunophenotyped using fluorochrome-conjugated mAbs (Table 1) as described [27]. Data was collected using a LSRII flow cytometer (band pass filters: 515/20 for FITC, 575/25 for PE, 675/40 for PerCP-Cy5.5 and 660/20 for APC). The relative percentages of cells were analyzed using FlowJo software.

2.6 Histological Analysis

Tissues were removed from euthanized mice and incubated overnight in neutral buffered (10%) formalin (Sigma-Aldrich). Fixed tissues were coated in paraffin, sectioned (5 µm) and stained with hematoxylin and eosin (POCD, Artarmon, Australia). Histological changes were assessed using a Leica (Wetzlar, Germany) DM IL inverted light microscope at 4× objective and images captured using a Motic (Causeway Bay, Hong Kong) Moticam 2 microscope camera and analyzed with Motic Images Plus software v2.0. Histological GVHD in the liver, skin, and GI tract was assessed, in a blinded fashion, using a standardized grading system (using grades from 0 to 4) as described [28].

2.7 Isolation of RNA and cDNA Synthesis

Tissues, removed from euthanized mice, were stored in RNAlater (Sigma-Aldrich) at -20°C until required. RNA was isolated using TRIzol reagent (Thermo Fisher Scientific) as per the manufacturer's instructions. Isolated RNA was immediately converted to complementary DNA (cDNA), using the qScript cDNA Synthesis Kit (Quanta Biosciences, Beverly, USA) as per the manufacturer's instructions, and stored at -80°C. cDNA quality was checked by PCR amplification of *hGAPDH/*murine (*m*)*Gapdh* (Invitrogen) and agarose gel electrophoresis as described [26].

2.8 Quantitative Real-time PCR (qPCR)

Quantitative real-time PCR (qPCR) reactions were performed using TaqMan Universal Master Mix II (Thermo Fisher Scientific) according to the manufacturer's instructions. qPCR was performed using primers for VIC-labelled m*Gapdh* (Mm99999915_g1) and human hypoxanthine-guanine phosphoribosyltransferase (h*HPRT-1*) (Hs02800695_m1), and FAM-labelled m*P2rx7* (Mm01199503_m1), h*P2RX7* (Hs00175721_m1) and h*IFNG* (Hs00989291_m1) (Thermo Fisher Scientific), as indicated. qPCR cycles consisted of two initial steps of 50°C for 2 min and 95°C for 10 min, and 40 cycles of 95°C for 15 s and 60°C for 1 min. qPCR reactions were conducted in triplicate, and were performed on a Roche Diagnostics (Indianapolis, USA) LightCycler 480, and analyses were conducted using LightCycler480 software v1.5.1.

2.9 Intracellular Staining

Splenocytes, following ammonium chloride potassium buffer lysis, were incubated for 4 h in RPMI 1640 medium containing 2 mM L-glutamine, 10% FCS, 1% non-essential amino acids (Thermo Fisher Scientific), 55 µM β-mercaptoethanol (Thermo Fisher Scientific), 100 U/mL penicillin and 100 µg/mL streptomycin (Thermo Fisher Scientific), 50 ng/mL phorbol 12-myristate 13-acetate (Sigma-Aldrich), 1 µg/mL ionomycin (Sigma-Aldrich), and 1 µg/mL GolgiStop™ (BD Biosciences). Cells were centrifuged (300 × *g* for 5 min) and washed once with PBS (300 × *g* for 5 min). Staining was performed using the BD Biosciences Intracellular Stain Kit as per the manufacturer's instructions and data were collected using a LSRII flow cytometer (band-pass filters: 515/20 for FITC, 575/25 for

PE, 675/40 for PerCP-Cy5.5 and 660/20 for APC). The percentage of hIFN-γ^+ and hIL-17^+ cells was analyzed using FlowJo software.

2.10 Enzyme-linked Immunosorbent Assay (ELISA)

Blood was collected via cardiac puncture from euthanized mice, incubated for 1 h at room temperature and centrifuged (1,700 × *g* for 10 min). Supernatants were centrifuged (1,700 × *g* for 10 min) and sera stored at -80°C. Serum cytokine concentrations were measured using a hIFN-γ Ready-Set-Go! ELISA Kit (eBioscience, San Diego, USA) as per the manufacturer's instructions. Absorbances (450 and 570 nm) were measured using a SpectraMax (Molecular Devices, Sunnyvale, USA) Plus 384 spectrophotometer.

2.11 Statistical Analyses

Data is given as mean ± standard error of the mean (SEM). All data sets were analyzed for normality (Shapiro-Wilk) and statistical differences were calculated using a paired or unpaired two-tailed Student's t test (parametric) or Mann–Whitney test (non-parametric) for single comparisons, or one-way analysis of variance (ANOVA) with a Tukey's post-hoc test for multiple comparisons. Weight and clinical score were analyzed using a repeated measures two-way ANOVA. Survival (median survival time; MST) was compared using the log-rank (Mantel-Cox) test and mortality was compared using the Fisher's exact test. All statistical analyses and graphs were generated using GraphPad Prism 5 (GraphPad Software, La Jolla, USA). $P < 0.05$ was considered significant for all tests.

3. Results

3.1 AZ10606120 Inhibits ATP-induced Cation Dye Uptake into Human and Murine Leukocytes

To confirm that AZ10 can block hP2X7 and mP2X7, human RPMI 8226 multiple myeloma and murine RAW 264.7 macrophage cells, both of which express endogenous P2X7 [29, 30], were pre-incubated with increasing concentrations of AZ10 followed by incubation with YO-PRO-1^{2+} and ATP. ATP-induced YO-PRO-1^{2+} uptake was assessed by flow cytometry. AZ10 exhibited a concentration-dependent inhibition of ATP-induced YO-PRO-1^{2+} uptake, with maximal inhibition at 1 μM in both cell types, and IC_{50} values of 3 ± 1 nM and 1 ± 1 nM in RPMI 8226 cells and RAW 264.7 cells, respectively (Figure 1a). These IC_{50} values are similar to published values for recombinant hP2X7 and mP2X7 [31].

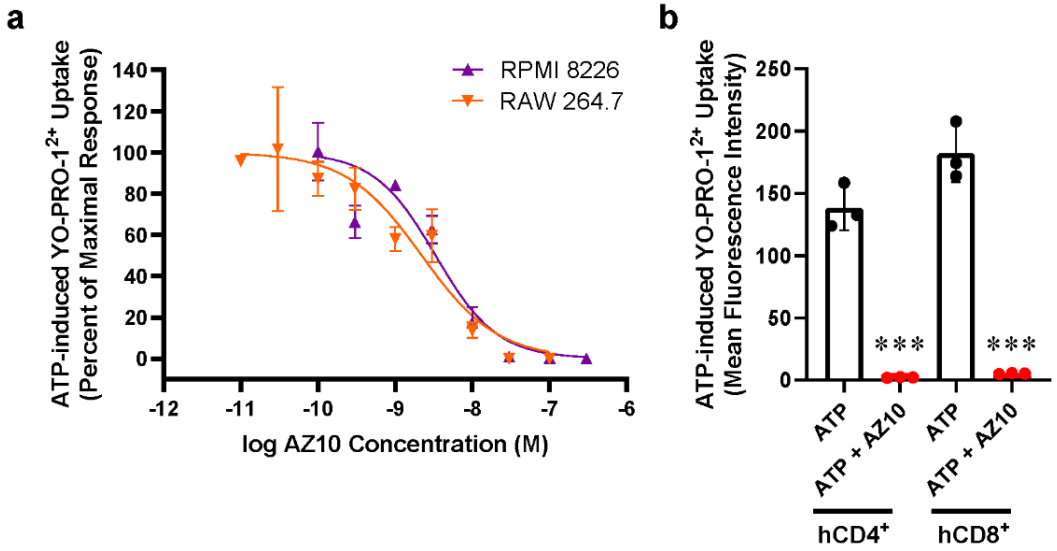

Figure 1 AZ10606120 (AZ10) prevents adenosine 5'-triphosphate (ATP)-induced cation dye uptake into human and murine leukocytes. (a) Human RPMI 8226 multiple myeloma cells, murine RAW264.7 macrophages, and (b) human peripheral blood mononuclear cells (hPBMCs) in NaCl medium were preincubated for 15 min at 37°C in the absence or presence of (a) AZ10 (as indicated) or (b) 100 nM AZ10. Cells were then incubated with 1 µM YO-PRO-1^{2+} in the absence or presence of 100 µM adenosine 5'-triphosphate (ATP) for 10 min at 37°C. YO-PRO-1^{2+} uptake into (a) RPMI 8226 or RAW 264.7 cells, and (b) hCD4$^+$ or hCD8$^+$ T cells was assessed by flow cytometry. (a) ATP-induced YO-PRO-1^{2+} uptake is represented as a percentage of maximal ATP response in the absence of AZ10. (b) ATP-induced YO-PRO-1^{2+} uptake is represented as mean fluorescence intensity. (a-b) Data represent group mean ± standard error of the mean (SEM) (n = 3). *** P < 0.001 to corresponding group with ATP.

To confirm that AZ10 can block P2X7 in donor hCD4$^+$ and hCD8$^+$ T cells, the main mediators of GVHD [32], hPBMCs were pre-incubated in the absence or presence of 100 nm AZ10 and ATP-induced YO-PRO-1^{2+} uptake was assessed as above. ATP induced YO-PRO-1^{2+} uptake into both hCD4$^+$ and hCD8$^+$ T cells, which were significantly reduced by 98.5% and 99.8%, respectively, by pre-incubation with AZ10 (P < 0.001, n = 3) (Figure 1b).

3.2 AZ10606120 Does Not Reduce Clinical Signs of GVHD in Humanized Mice

To determine if AZ10 can ameliorate disease development in a humanized mouse model of GVHD, NSG mice were injected i.p. with 10 × 10^6 hPBMCs and then with saline (vehicle control) or AZ10 (2 mg/kg) daily for 10 days (days 0-10) and monitored for signs of GVHD (Figure 2a). This AZ10 dose has been previously shown to mediate therapeutic effects in a murine model of depression [22]. The i.p. injection route has been repeatedly used for the administration of other P2X7 antagonists in mouse models of GVHD. All mice injected with either saline or AZ10 exhibited weight loss from 4 weeks, with similar weight loss between groups over the course of the study (P = 0.8720) (Figure 2b). Both groups of mice began to show signs of GVHD from day 35, and mice injected with either saline or AZ10 had similar clinical scores as the disease progressed (P = 0.6806) (Figure 2c). As such,

mortality and median survival time (MST) was similar between saline- and AZ10-injected mice (85% and 100% mortality, respectively, $P = 0.9882$; MST of 55 and 48 days, respectively, $P = 0.8022$) (Figure 2d).

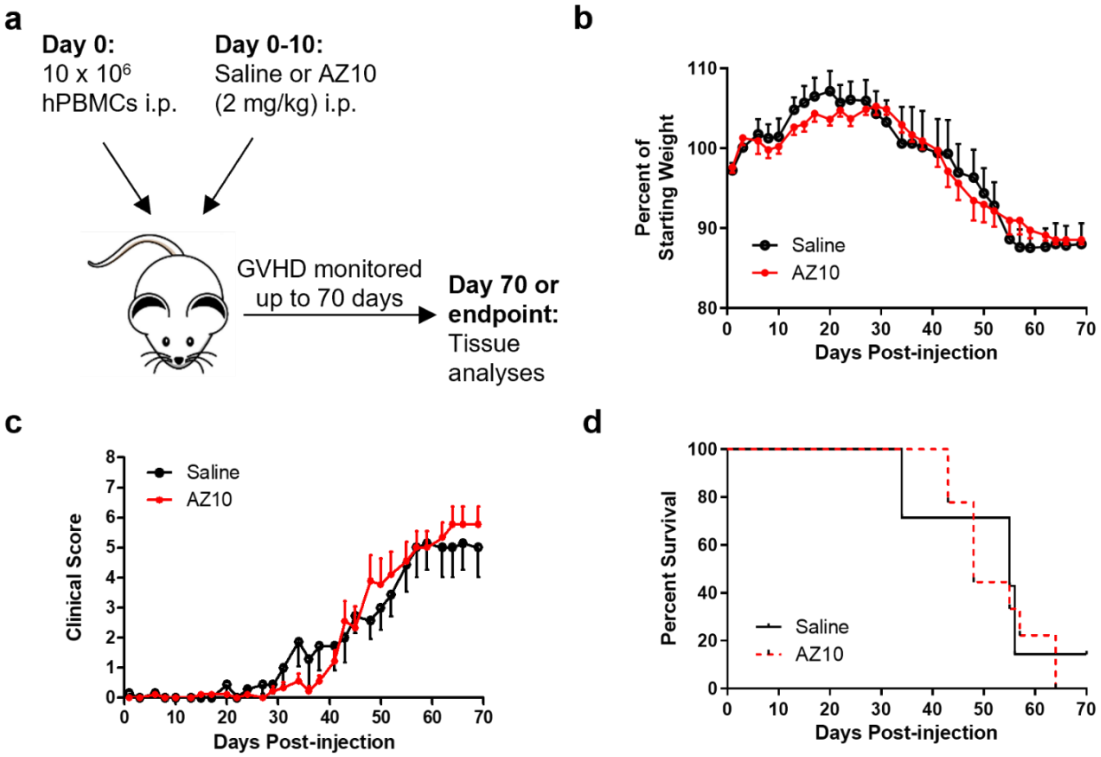

Figure 2 AZ10606120 (AZ10) does not prevent graft-versus-host disease (GVHD) in humanized mice. (a) Schematic representation of the humanized mouse model of GVHD. (a-e) NOD.Cg-*Prkdc*^{scid} *Il2rg*^{tm1Wjl}/SzJ (NSG) mice were injected intraperitoneally (i.p.) with 10 × 10^6 human peripheral blood mononuclear cells (hPBMCs) at day 0, then injected i.p. with saline ($n = 7$ mice) or 2 mg/kg AZ10 ($n = 8$ mice) daily (days 0-10). Mice were assessed thrice weekly for up to 70 days for (b) weight, (c) clinical score, and (d) survival. (b-c) Data presented as mean ± standard error of the mean (SEM).

3.3 AZ10606120 Does Not Prevent Histological GVHD in Humanized Mice

Engraftment of hPBMCs in NSG mice leads to leukocyte infiltration and damage to GVHD target tissues including liver and skin, with nil to minor histological changes observed in the GI tract [33]. Livers from mice demonstrated leukocyte infiltration and minor damage to hepatic triads. Livers from AZ10-injected mice demonstrated a mild reduction in these parameters compared to saline-injected mice, but this did not reach statistical significance (Figure 3a). Both saline- and AZ10-injected humanized mice demonstrated minor but similar epidermal thickening in the skin of some mice (Figure 3b). There was no histological evidence of GVHD in the GI tract of most mice (Figure 3c).

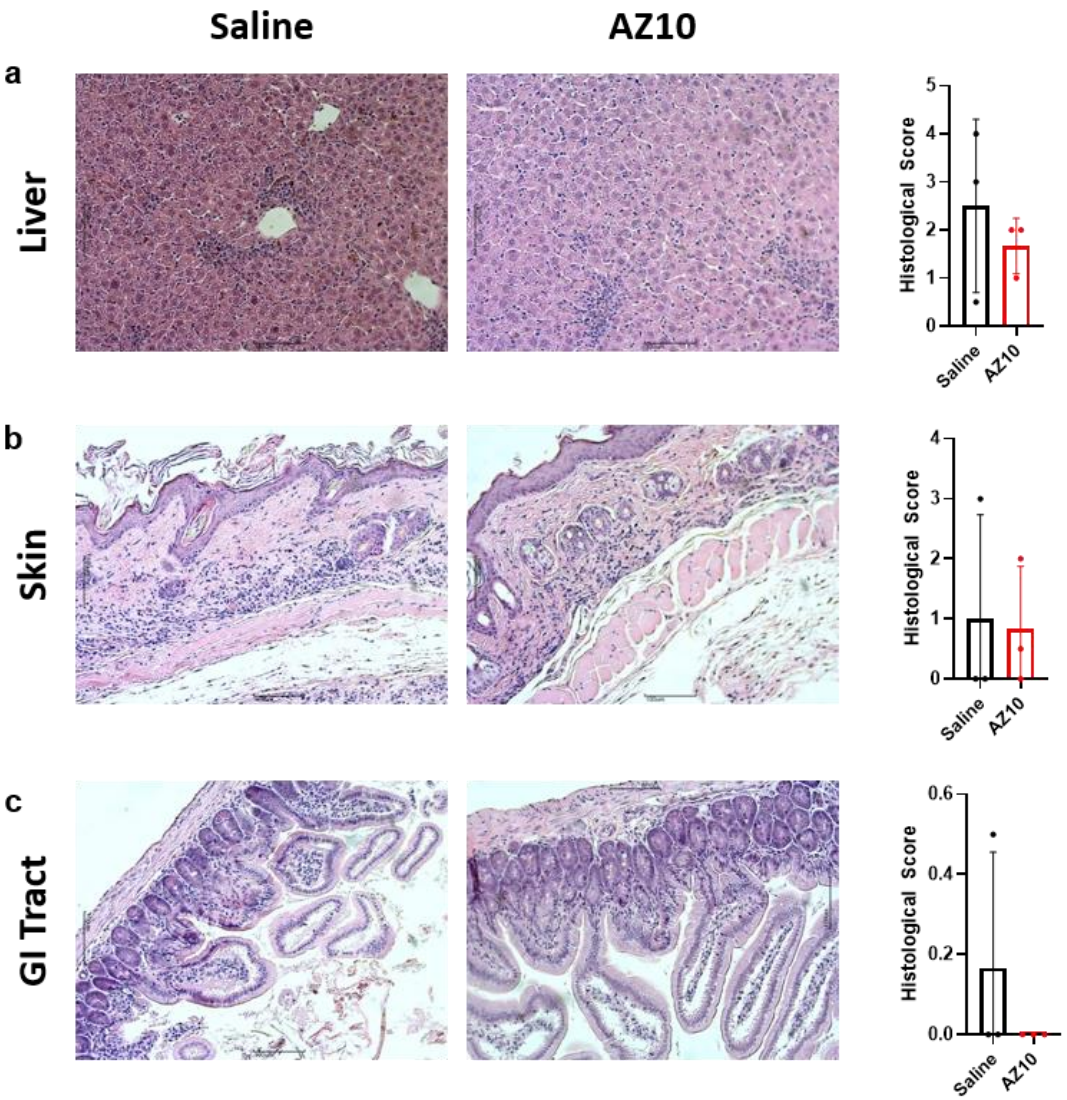

Figure 3 AZ10606120 (AZ10) does not prevent histological graft-versus-host disease (GVHD) in humanized mice. Sections of **(a)** liver, **(b)** skin, and **(c)** gastrointestinal (GI) tract from humanized mice treated with saline ($n = 3$) or AZ10 ($n = 3$) at endpoint were stained with hematoxylin and eosin, and graded to yield a histological GVHD score. (*Right panels*) Data presented as mean ± standard error of the mean (SEM).

3.4 AZ10606120 Does Not Affect hPBMC Engraftment in NSG Mice

To investigate if human cell engraftment was affected by AZ10 treatment, flow cytometric analysis of blood at 3 weeks post-hPBMC injection, and of spleens at endpoint was undertaken (Figure 4a). Analysis of blood at 3 weeks post-hPBMC injection demonstrated that both saline- and AZ10-injected mice had similar proportions of human leukocytes (21.8 ± 4.4% and 22.8 ± 3.9% $hCD45^+$ $mCD45^-$ cells, respectively; $P = 0.8623$) (Figure 4b). T cells comprised the majority of $hCD45^+$ cells with similar T cell proportions in saline- and AZ10-injected mice (97.0 ± 0.8% and 98.0 ± 0.4% $hCD3^+$ cells, respectively; $P = 0.2738$) (Figure 4c). The presence of NK cells ($hCD3^-$ $hCD56^+$) in all humanized mice was negligible in both groups (data not shown). However, in all mice there was a small population of $hCD3^+$ $hCD56^+$ cells, representing either activated T cells [34] or natural killer T

cells [35] or both, but the proportions of these cells did not vary between saline- and AZ10-injected mice (0.8 ± 0.3% and 1.3 ± 0.3% hCD3$^+$ hCD56$^+$ cells, respectively; $P = 0.2462$) (Figure 4d).

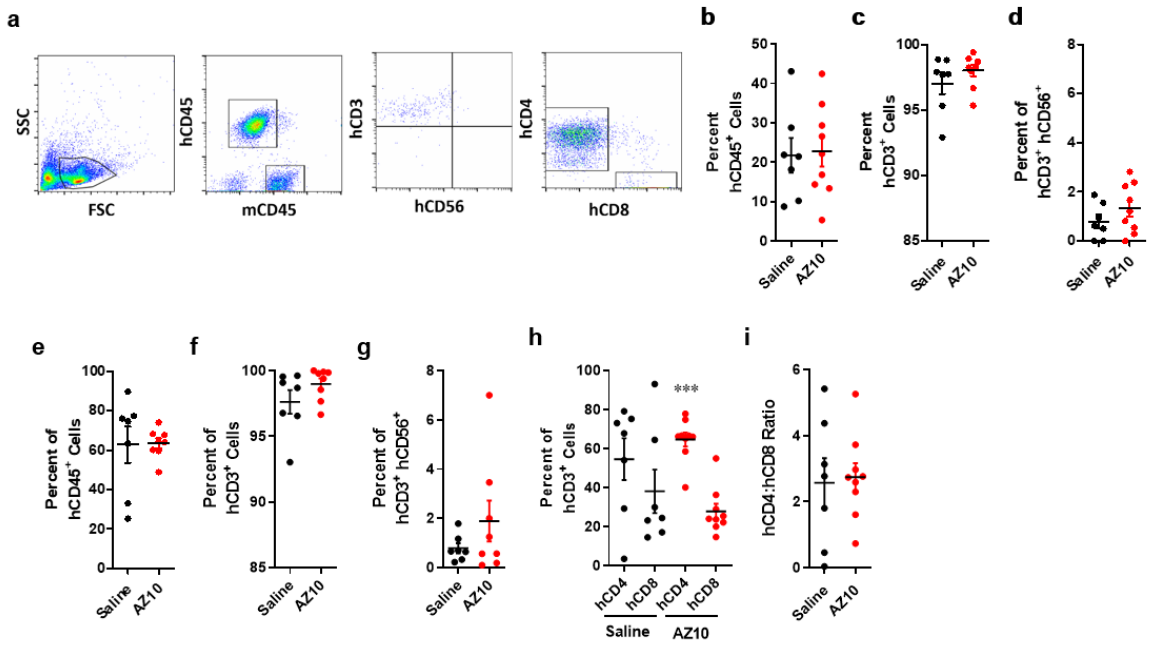

Figure 4 AZ10606120 (AZ10) does not affect engraftment of human cells. (a-d) Blood (3 weeks post-human (h) peripheral blood mononuclear cell (hPBMC) injection) and (e-i) spleens (endpoint) from humanized mice treated with saline ($n = 7$) or AZ10 ($n = 9$) were examined by flow cytometry to identify human cell populations at endpoint. (a) Example of the flow cytometric gating strategy used to identify lymphocytes using FSC vs SSC (*far left panel*), human leukocytes (*middle left panel*) and subsequently T cells (*middle right panel*), and T cell subsets (*far right panel*) to determine the proportion of (b, e) hCD45$^+$ (mCD45$^-$), (c, f) hCD3$^+$, (d, g) hCD3$^+$ hCD56$^+$, and (h) hCD4$^+$ and hCD8$^+$ cells, and the (i) hCD4:hCD8 ratio. Data represents group mean ± standard error of the mean (SEM); symbols represent individual mice; ***$P < 0.001$ compared to corresponding hCD8$^+$ T cells.

Splenocyte analysis at endpoint demonstrated human leukocytes comprised the majority of total murine and human leukocytes, with proportions similar in saline- and AZ10- injected mice (62.8 ± 9.1% and 63.4 ± 2.6% hCD45$^+$ mCD45$^-$ cells, respectively; $P = 0.9485$) (Figure 4e). Similar to engraftment at 3 weeks post-hPBMC injection, T cells comprised the majority of human leukocytes and proportions were similar between saline- and AZ10-injected mice (97.6 ± 0.9% and 99.0 ± 0.4% hCD3$^+$ cells, respectively; $P = 0.1520$) (Figure 4f). Again, the percentage of NK cells (hCD3$^-$ hCD56$^+$) was negligible in both groups (data not shown). In all mice there was a small population of hCD3$^+$ hCD56$^+$ cells, but the percentage of these cells did not vary between saline- and AZ10-injected mice (0.8 ± 0.2% and 1.9 ± 0.8% hCD3$^+$ hCD56$^+$ cells, respectively) ($P = 0.7789$) (Figure 4g).

Human T cell analysis (hCD3$^+$) in spleens at endpoint revealed that saline- and AZ10-injected mice demonstrated similar proportions of hCD4$^+$ T cells (54.7 ± 10.7% and 64.7 ± 3.6%, respectively; $P = 0.3398$) and hCD8$^+$ T cells (38.1 ± 11.1% and 27.9 ± 3.9%, respectively; $P = 0.3521$) (Figure 4h). AZ10-injected, but not saline-injected, mice demonstrated significantly higher engraftment of hCD4$^+$ T

cells than hCD8$^+$ T cells ($P < 0.0001$ and $P = 0.3055$, respectively) (Figure 4h). However, the mean hCD4:hCD8 T cell ratio was not significantly different between saline- and AZ10-injected mice (2.9 ± 0.6 and 3.4 ± 1.0, respectively; $P = 0.8353$) (Figure 4i).

3.5 AZ10606120 Does Not Alter Splenic Human or Mouse P2X7 Expression

P2X7 expression can be increased in some tissues in allogeneic and humanized mouse models of GVHD [7, 33]. Spleens from saline- and AZ10-injected mice, were analyzed for m*P2rx7* and h*P2RX7* expression. Mean relative m*P2X7* expression was similar between saline- and AZ10-injected mice (0.8 ± 0.2 and 0.7 ± 0.2, respectively; $P = 0.7096$) (Figure 5a). Conversely, mean relative h*P2RX7* expression was 2.5-fold higher in AZ10-injected mice compared to saline-injected mice (2 ± 2 and 0.9 ± 0.1, respectively; $P = 0.9998$) (Figure 5b), but this difference was due to one AZ10-injected mouse exhibiting relatively high relative h*P2RX7* expression compared to all other mice.

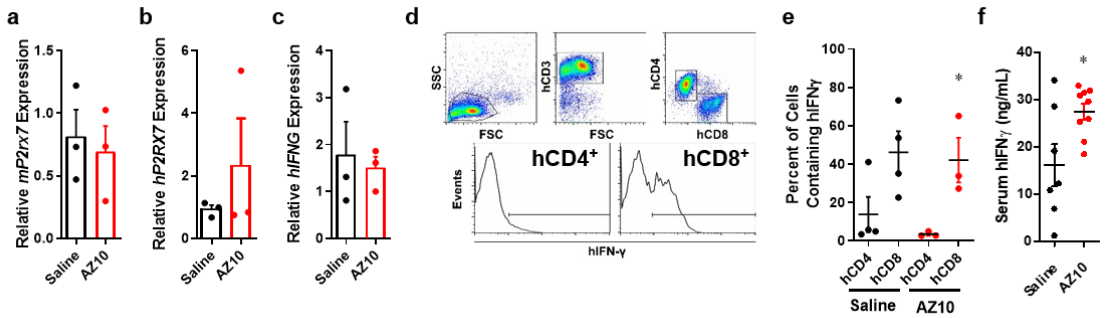

Figure 5 AZ10606120 (AZ10) increases serum human interferon (hIFN)-γ in humanized mice. (a-c) Complementary DNA (cDNA) from spleens from humanized mice injected with saline ($n = 3$) or AZ10 ($n = 3$) at endpoint was used to assess the relative expression of (a) murine (m) *P2rx7* (b) human (h) *P2RX7* and (c) *hIFNG* expression by quantitative real-time polymerase chain reaction (qPCR). (d-e) Splenocytes from humanized mice injected with saline ($n = 3$) or AZ10 ($n = 4$) at endpoint were incubated with phorbol 12-myristate 13-acetate (PMA), ionomycin and Golgi-stop for 4 h. (d) Flow cytometry was used to initially identify lymphocytes using FSC vs SSC (*top left panel*) and then hCD3$^+$ T cells (*top middle panel*) to determine the percentage of hCD4$^+$ and hCD8$^+$ T cells (*top right panel*) producing intracellular hIFN-γ (*bottom panels; hCD4$^+$ left, hCD8$^+$ right*) and (e) proportions of hIFN-γ$^+$ subsets. *$P < 0.05$ compared to corresponding hCD4$^+$ T cells. (f) Concentrations of serum hIFN-γ from humanized mice injected with saline ($n = 7$) or AZ10 ($n = 9$) at endpoint were analyzed by ELISA. Data represents group means ± SEM; symbols represent individual mice. *$P < 0.05$.

3.6 AZ10606120 Increases Serum Human IFN-γ in Humanized Mice

IFN-γ is an important pro-inflammatory cytokine implicated in the pathogenesis of GVHD [36], and the non-selective P2X7 antagonist BBG reduces serum hIFN-γ in humanized mice [10, 11]. Spleens from saline- and AZ10-injected mice, were analyzed for relative *hIFNG* expression. Relative

hIFNG expression in the spleens of AZ10-injected mice was similar to that of saline-injected mice (1.5 ± 0.3 and 1.8 ± 0.7, respectively; $P = 0.7360$) (Figure 5c).

Flow cytometric analysis of intracellular hIFN-γ in splenocytes revealed both $hCD4^+$ and $hCD8^+$ T cells produced IFN-γ, with IFN-γ production in each respective subset similar between saline- and AZ10-injected mice ($hCD4^+$ T cells, $P = 0.3823$; $hCD8^+$ T cells $P = 0.8129$) (Figure 5d). Notably, IFN-γ production was 3.5-fold greater in $hCD8^+$ cells compared to $hCD4^+$ T cells within saline-injected mice (46 ± 19% and 13 ± 7%, respectively; $P = 0.0648$). Further there was 10.5-fold greater IFN-γ production within $hCD8^+$ cells compared to $hCD4^+$ T cells within AZ10-injected mice (42.3 ± 7.2% and 4.2. ± 2.8%, respectively; $P = 0.0298$) (Figure 5e). Finally, serum hIFN-γ concentrations in mice were assessed by ELISA. hIFN-γ was present in the serum of all mice for which samples were available. Serum hIFN-γ was significantly increased 1.8-fold in AZ10-injected mice compared to saline-injected mice (27.5 ± 1.7 ng/mL and 16.2 ± 4.5 ng/mL, respectively; $P = 0.0207$) (Figure 5f).

4. Discussion

The major finding of the current study is that the selective P2X7 antagonist AZ10 did not reduce GVHD in humanized mice. This result contrasts with previous findings using the non-selective P2X7 antagonist BBG, which reduced clinical and histological GVHD in humanized mice [10, 11, 37]. Reasons for these differences remain unknown. AZ10 was used at a dose of 2 mg/kg, which has proven efficacy in mice [22] but is 25-times lower than the dose of BBG (50 mg/kg) that reduced GVHD in this same humanized mouse model [10, 11, 37]. However, comparison of similarly designed *in vitro* studies reveals that AZ10 is approximately 100- and 20-times more potent at antagonizing human and murine P2X7 (this study), compared to BBG [10], with IC_{50} values of 1 and 3 nM for AZ10, versus IC_{50} values of 100 and 60 nM for BBG, against human and murine P2X7, respectively. Thus, although not compared directly at the same time, the AZ10 dose used in the current study is unlikely to explain the differences observed between AZ10 and BBG in reducing GVHD. Furthermore, the AZ10 injection regime used (daily, days 0-10) is the same as that previously used for BBG to reduce GVHD (daily, days 0-10) [11] and therefore is also unlikely to explain the differences observed between AZ10 and BBG. Nevertheless, the possibility remains that a higher dose of AZ10 may be able to reduce GVHD in humanized mice. The possibility also exists that AZ10 and BBG have different pharmacokinetics, which may explain the differences on GVHD development between these two compounds in humanized mice. In this regard, BBG remains highly visible at the injection site and in tissues of humanized mice at endpoint [11], but whether it retains its inhibitory activity throughout the model, especially at later time points when clinical disease is evident, remains unknown. Thus, future studies should explore the impact of long-term regimes with P2X7 antagonists, including AZ10, in preventing GVHD development in mice. A final explanation for the differences observed between AZ10 and BBG in reducing GVHD may relate to differences in specificity. AZ10 is a highly specific P2X7 antagonist [15-17]. In contrast, BBG also impairs P2X1 [38] and P2X4 [39], both which are present on APCs [40] and T cells [41]. Therefore, BBG may reduce GVHD by blocking P2X receptors in addition to P2X7 to reduce ATP-induced signaling events in murine APCs or human T cells, which would normally act to promote GVHD. The role of other P2X receptors in GVHD however remains to be reported. In addition, BBG can impair the ATP release channel pannexin-1 [42]. Thus, BBG may also reduce GVHD by blocking ATP release and subsequent activation of P2X7, potentially acting as a dual antagonist of the ATP-P2X7 signaling axis.

Despite not impacting GVHD development, AZ10 increased serum hIFN-γ in humanized mice. This result contrasts previous findings with BBG, which reduced serum hIFN-γ and was associated with a reduction in GVHD in this model [10, 11]. The role of hIFN-γ in the humanized NSG model of GVHD remains unknown, but increased serum hIFN-γ is associated with more severe GVHD in this model [26] and use of other therapies that reduce GVHD in this same model corresponds with a reduction in serum hIFN-γ [43, 44]. Collectively, these studies support the notion that hIFN-γ contributes to GVHD progression. Notably, the increased serum hIFN-γ observed with AZ10 treatment did not worsen GVHD in mice, with arguably a slight reduction in histological GVHD in the liver of mice treated with AZ10. Nevertheless, it remains unknown why AZ10 increased serum hIFN-γ in the current study. qRT-PCR revealed that expression of *hIFNG* mRNA in the spleens was similar between saline- and AZ10-treated mice. Moreover, intracellular staining of human T cells at endpoint revealed the presence of both IFN-γ^+ $CD4^+$ and IFN-γ^+ $CD8^+$ T cells and that the relative proportion of IFN-γ^+ cells in either subset was not affected by AZ10. Notably, the proportion of IFN-γ^+ $CD8^+$ T cells was increased compared IFN-γ^+ $CD4^+$ T cells in AZ10-treated but not saline-treated mice, suggesting that AZ10 may be increasing the total number of IFN-γ^+ $CD8^+$ T cells, which are likely to be predominantly memory $CD8^+$ T cells based on other observations in this model [45]. This finding however, appears at odds with the emerging role of P2X7 activation in promoting the long-term survival of memory human $CD8^+$ T cells *in vitro* [46], with P2X7 blockade predicted to reduce $CD8^+$ T cells. Furthermore, to the best of our knowledge the effect of P2X7 blockade on IFN-γ production in human $CD8^+$ T cells has not been reported, but P2X7 blockade can reduce IFN-γ production in murine $CD8^+$ T cells isolated from lung allografts [47]. In contrast, P2X7 blockade does not appear to affect the development of human IFN-γ^+ $CD4^+$ T cells *in vitro* [48], which is consistent with the similar proportions of this cell type in saline- and AZ10-trated humanized mice.

Finally, qRT-PCR revealed that expression of h*P2RX7* and m*P2rx7* mRNA in the spleens were similar between saline- and AZ10-treated mice. P2X7 can be up-regulated in humanized [33] or allogeneic mouse models of GVHD, as well as in allo-HSCT recipients with GVHD [7]. Thus, this data in the current study supports the notion that AZ10 had little impact on GVHD development in humanized mice.

A limitation of the current study is that the GVHD model was restricted to the use of one hPBMC donor. However, P2X7 antagonism with BBG has previously shown efficacy against hPBMCs from this donor in the development of hepatic GVHD and production of serum IFN-γ in NSG mice [10], while AZ10 was shown to impair ATP-induced YO-PRO-1^{2+} uptake into human $CD4^+$ and $CD8^+$ T cells from this donor in the current study. Another limitation was that human $CD4^+$ T regulatory cells (hTregs) were not investigated. Previous studies have revealed that P2X7 antagonism with PPADS or BBG can reduce GVHD and that this effect corresponds with an increase in donor Tregs in both allogeneic [7] and humanized [11] mouse models. A final limitation of the current study, as alluded to above, is that the pharmacokinetics of AZ10 in NSG mice is unknown and the possibility remains that mice were not sufficiently dosed to fully block P2X7. Nonetheless, in accordance with the expectations of our animal ethics committee, it is important to present this current data to assist in the use of AZ10 and other P2X7 antagonists in future *in vivo* models of GVHD or other diseases.

Finally, it needs to be noted that while humanized (xenogeneic) mouse models of GVHD provide valuable insights into the role of human immune cells in GVHD [49], they do not fully recapitulate human GVHD nor allogeneic mouse models of this disease as explained in detail elsewhere [50]. In brief, humanized mouse models are less prone to GI GVHD, the main cause of mortality in humans

and allogeneic mice with GVHD, but are more prone to liver and lung GVHD, which typically determine the ethical endpoint in these xenogeneic models of GVHD. Moreover, injection of NSG mice with hPBMCs largely results in human T cell engraftment (as observed in the current study), while their activation by donor and/or host APCs remains poorly understood. Thus, the lack of efficacy of AZ10 in the current study, compared to the use of other specific P2X7 antagonists in allogeneic mouse models of GVHD [7, 8], could possibly be attributed to differences in tissue-specific GVHD development and/or donor T cell activation by APCs.

5. Conclusions

In conclusion, the current study revealed that the specific P2X7 antagonist AZ10 (2 mg/kg i.p. daily, days 0-10) did not reduce GVHD in this model and unexpectedly increased serum hIFN-γ. Thus, direct evidence beyond the use of BBG is required to confirm a role for P2X7 activation in the NSG mouse model of GVHD.

Acknowledgments

The authors thank the staff of the Illawarra Health and Medical Research Institute, and the Molecular Horizons Fluorescence Analysis Facility and Molecular Horizons Animal Research Facility for technical assistance.

Author Contributions

N.J.G., D.W. and R.S. designed the experiments. N.J.G., A.E., P.C. and R.S. performed the experiments and analyzed the data. D.W. and R.S. supervised the project and reviewed the data. N.J.G. prepared the figures and drafted the manuscript. All authors reviewed and edited the manuscript.

Funding

This project was funded by a Faculty of Science, Medicine and Health grant and a RevITAlise (RITA) Team grant, both from the University of Wollongong, and a Cancer Council NSW project grant. N.J.G. is currently supported by the Motor Neurone Disease Research Australia Marisa Aguis Post-doctoral fellowship. D.W is currently supported by a COVID-impacted Emerging Research Leadership (CERL) fellowship from the University of Wollongong. A.E. and P.C. are supported by Australian Government Research Training Program Scholarships.

Competing Interests

All authors declare that they have no competing interests.

References

1. Copelan EA. Hematopoietic stem-cell transplantation. N Engl J Med. 2006; 354: 1813-1826.
2. Zeiser R, Blazar BR. Acute graft-versus-host disease—biologic process, prevention, and therapy. N Engl J Med. 2017; 377: 2167-2179.

3. Sharma N, Efebera Y. Acute graft-versus-host disease, prophylaxis and therapy. OBM Transplant. 2021; 5: 139.
4. Geraghty NJ, Watson D, Adhikary SR, Sluyter R. P2X7 receptor in skin biology and diseases. World J Dermatol. 2016; 5: 72-83.
5. Hill GR, Betts BC, Tkachev V, Kean LS, Blazar BR. Current concepts and advances in graft-versus-host disease immunology. Ann Rev Immunol. 2021; 39: 19-49.
6. Cuthbertson P, Geraghty NJ, Adhikary SR, Bird KM, Fuller SJ, Watson D, et al. Purinergic signalling in allogeneic haematopoietic stem cell transplantation and graft-versus-host disease. Int J Mol Sci. 2021; 22: 8343.
7. Wilhelm K, Ganesan J, Müller T, Dürr C, Grimm M, Beilhack A, et al. Graft-versus-host disease is enhanced by extracellular ATP activating P2X7R. Nat Med. 2010; 16: 1434-1438.
8. Koehn BH, Saha A, McDonald-Hyman C, Loschi M, Thangavelu G, Ma L, et al. Danger-associated extracellular ATP counters MDSC therapeutic efficacy in acute GvHD. Blood. 2019; 134: 1670-1682.
9. Sluyter R, Watson D. Use of humanized mouse models to investigate the roles of purinergic signaling in inflammation and immunity. Front Pharmacol. 2020; 11: 596357.
10. Geraghty NJ, Belfiore L, Ly D, Adhikary SR, Fuller SJ, Varikatt W, et al. The P2X7 receptor antagonist Brilliant Blue G reduces serum human interferon-γ in a humanized mouse model of graft-versus-host disease. Clin Exp Immunol. 2017; 190: 79-95.
11. Cuthbertson P, Geraghty NJ, Adhikary SR, Casolin S, Watson D, Sluyter R. P2X7 receptor antagonism increases regulatory T cells and reduces clinical and histological graft-versus-host disease in a humanised mouse model. Clin Sci. 2021; 135: 495-513.
12. Covarrubias R, Chepurko E, Reynolds A, Huttinger ZM, Huttinger R, Stanfill K, et al. Role of the CD39/CD73 purinergic pathway in modulating arterial thrombosis in mice. Arterioscler Thromb Vasc Biol. 2016; 36: 1809-1820.
13. Geraghty NJ, Watson D, Sluyter R. Pharmacological blockade of the CD39/CD73 pathway but not adenosine receptors augments disease in a humanized mouse model of graft-versus-host disease. Immunol Cell Biol. 2019; 97: 597-610.
14. Sluyter R. The P2X7 receptor. Adv Exp Med Biol. 2017; 1051: 17-53.
15. Michel AD, Chambers LJ, Clay WC, Condreay JP, Walter DS, Chessell IP. Direct labelling of the human P2X7 receptor and identification of positive and negative cooperativity of binding. Br J Pharmacol. 2007; 151: 84-95.
16. Michel AD, Chambers LJ, Walter DS. Negative and positive allosteric modulators of the P2X7 receptor. Br J Pharmacol. 2008; 153: 737-750.
17. Allsopp RC, Dayl S, Schmid R, Evans RJ. Unique residues in the ATP gated human P2X7 receptor define a novel allosteric binding pocket for the selective antagonist AZ10606120. Sci Rep. 2017; 7: 725.
18. Karasawa A, Kawate T. Structural basis for subtype-specific inhibition of the P2X7 receptor. eLife. 2016; 5: e22153.
19. Allsopp RC, Dayl S, Bin Dayel A, Schmid R, Evans RJ. Mapping the allosteric action of antagonists A740003 and A438079 reveals a role for the left flipper in ligand sensitivity at P2X7 receptors. Mol Pharmacol. 2018; 93: 553-562.

20. Bin Dayel A, Evans RJ, Schmid R. Mapping the site of action of the human P2X7 receptor antagonists AZ11645373, Brilliant Blue G, KN-62, calmidazolium and ZINC58368839 to the inter-subunit allosteric pocket. Mol Pharmacol. 2019; 96: 355-363.
21. Pupovac A, Stokes L, Sluyter R. CAY10593 inhibits the human P2X7 receptor independently of phospholipase D1 stimulation. Purinergic Signal. 2013; 9: 609-619.
22. Csölle C, Baranyi M, Zsilla G, Kittel Á, Gölöncsér F, Illes P, et al. Neurochemical changes in the mouse hippocampus underlying the antidepressant effect of genetic deletion of P2X7 receptors. PLOS One. 2013; 8: e66547.
23. Giannuzzo A, Saccomano M, Napp J, Ellegaard M, Alves F, Novak I. Targeting of the P2X7 receptor in pancreatic cancer and stellate cells. Int J Cancer. 2016; 139: 2540-2552.
24. Pupovac A, Geraghty NJ, Watson D, Sluyter R. Activation of the P2X7 receptor induces the rapid shedding of CD23 from human and murine B cells. Immunol Cell Biol. 2015; 93: 77-85.
25. Geraghty NJ, Mansfield KJ, Fuller SJ, Watson D, Sluyter R. The P2X7 receptor is not essential for development of imiquimod-induced psoriasis-like inflammation in mice. Purinergic Signal. 2017; 13: 405-415.
26. Geraghty NJ, Belfiore L, Adhikary SR, Alexander SI, Sluyter R, Watson D. Increased splenic human $CD4^+$:$CD8^+$ T cell ratios, serum human interferon-γ and intestinal human interleukin-17 are associated with clinical graft-versus-host disease in humanized mice. Transpl Immunol. 2019; 54: 38-46.
27. Geraghty NJ, Adhikary SR, Watson D, Sluyter R. The A2A receptor agonist CGS 21680 has beneficial and adverse effects on disease development in a humanised mouse model of graft-versus-host disease. Int Immunopharmacol. 2019; 72: 479-486.
28. Hu M, Hawthorne WJ, Nicholson L, Burns H, Qian YW, Liuwantara D, et al. Low-dose interleukin-2 combined with rapamycin led to an expansion of $CD4^+CD25^+FOXP3^+$ regulatory T cells and prolonged human islet allograft survival in humanized mice. Diabetes. 2020; 69: 1735-1748.
29. Farrell AW, Gadeock S, Pupovac A, Wang B, Jalilian I, Ranson M, et al. P2X7 receptor activation induces cell death and CD23 shedding in human RPMI 8226 multiple myeloma cells. Biochim Biophys Acta Gen Subj. 2010; 1800: 1173-1182.
30. Sperlágh B, Haskó G, Németh Z, Vizi ES. ATP released by LPS increases nitric oxide production in raw 264.7 macrophage cell line via P2Z/P2X7 receptors. Neurochem Int. 1998; 33: 209-215.
31. Bartlett R, Stokes L, Sluyter R. The P2X7 receptor channel: Recent developments and the use of P2X7 antagonists in models of disease. Pharmacol Rev. 2014; 66: 638-675.
32. King MA, Covassin L, Brehm MA, Racki W, Pearson T, Leif J, et al. Human peripheral blood leucocyte non-obese diabetic-severe combined immunodeficiency interleukin-2 receptor gamma chain gene mouse model of xenogeneic graft-versus-host-like disease and the role of host major histocompatibility complex. Clin Exp Immunol. 2009; 157: 104-118.
33. Cuthbertson P, Adhikary SR, Geraghty NJ, Guy TV, Hadjiashrafi A, Fuller SJ, et al. Increased P2X7 expression in the gastrointestinal tract and skin in a humanised mouse model of graft-versus-host disease. Clin Sci. 2020; 134: 207-223.
34. Kelly-Rogers J, Madrigal-Estebas L, O'Connor T, Doherty DG. Activation-induced expression of CD56 by T cells is associated with a reprogramming of cytolytic activity and cytokine secretion profile in vitro. Hum Immunol. 2006; 67: 863-873.

35. Ortaldo JR, Winkler-Pickett RT, Yagita H, Young HA. Comparative studies of $CD3^-$ and $CD3^+$ $CD56^+$ cells: Examination of morphology, functions, T cell receptor rearrangement, and pore-forming protein expression. Cell Immunol. 1991; 136: 486-495.
36. Yi T, Chen Y, Wang L, Du G, Huang D, Zhao D, et al. Reciprocal differentiation and tissue-specific pathogenesis of Th1, Th2, and Th17 cells in graft-versus-host disease. Blood. 2009; 114: 3101-3112.
37. Geraghty NJ, Watson D, Sluyter R. Long-term treatment with the P2X7 receptor antagonist Brilliant Blue G reduces liver inflammation in a humanized mouse model of graft-versus-host disease. Cell Immunol. 2019; 336: 12-19.
38. Seyffert C, Schmalzing G, Markwardt F. Dissecting individual current components of co-expressed human P2X1 and P2X7 receptors. Curr Top Med Chem. 2004; 4: 1719-1730.
39. Jiang L-H, Mackenzie AB, North RA, Surprenant A. Brilliant blue G selectively blocks ATP-gated rat P2X7 receptors. Mol Pharmacol. 2000; 58: 82-88.
40. Berchtold S, Ogilvie AL, Bogdan C, Muhl-Zurbes P, Ogilvie A, Schuler G, et al. Human monocyte derived dendritic cells express functional P2X and P2Y receptors as well as ecto-nucleotidases. FEBS Lett. 1999; 458: 424-428.
41. Woehrle T, Yip L, Elkhal A, Sumi Y, Chen Y, Yao Y, et al. Pannexin-1 hemichannel–mediated ATP release together with P2X1 and P2X4 receptors regulate T-cell activation at the immune synapse. Blood. 2010; 116: 3475-3484.
42. Qiu F, Dahl G. A permeant regulating its permeation pore: Inhibition of pannexin 1 channels by ATP. Am J Physiol Cell Physiol. 2009; 296: 250-255.
43. Gregoire-Gauthier J, Durrieu L, Duval A, Fontaine F, Dieng MM, Bourgey M, et al. Use of immunoglobulins in the prevention of GvHD in a xenogeneic NOD/SCID/γc- mouse model. Bone Marrow Transplant. 2012; 47: 439-450.
44. Ehx, Fransolet G, de Leval L, D'Hondt S, Lucas S, Hannon M, et al. Azacytidine prevents experimental xenogeneic graft-versus-host disease without abrogating graft-versus-leukemia effects. OncoImmunology. 2017; 6: e1314425.
45. Adhikary SR, Cuthbertson P, Nicholson L, Bird KM, Sligar C, Hu M, et al. Post-transplant cyclophosphamide limits reactive donor T cells and delays the development of graft-versus-host disease in a humanized mouse model. Immunology. 2021; 164: 332-347.
46. Borges da Silva H, Beura LK, Wang H, Hanse EA, Gore R, Scott MC, et al. The purinergic receptor P2RX7 directs metabolic fitness of long-lived memory $CD8^+$ T cells. Nature. 2018; 559: 264-268.
47. Liu K, Vergani A, Zhao P, Ben Nasr M, Wu X, Iken K, et al. Inhibition of the purinergic pathway prolongs mouse lung allograft survival. Am J Respir Cell Mol Biol. 2014; 51: 300-310.
48. Hamoudi C, Zhao CQ, Abderrazak A, Salem M, Fortin PR, Sevigny J, et al. The purinergic receptor P2X4 promotes Th17 activation and the development of arthritis. J Immunol. 2022; 208: 1115-1127.
49. Shultz LD, Keck J, Burzenski L, Jangalwe S, Vaidya S, Greiner DL, et al. Humanized mouse models of immunological diseases and precision medicine. Mamm Genome. 2019; 30: 123-142.
50. Koyama M, Hill GR. Mouse models of antigen presentation in hematopoietic stem cell transplantation. Front Immunol. 2021; 12: 715893.

Enjoy *OBM Transplantation* by:

1. Submitting a manuscript
2. Joining in volunteer reviewer bank
3. Joining Editorial Board
4. Guest editing a special issue

For more details, please visit:
http://www.lidsen.com/journals/transplantation